Primljen / Received: 15.11.2025.
Ispravljen / Corrected: 5.12.2025.
Prihvaćen / Accepted: 8.12.2025.
Dostupno online / Available online: 15.12.2025.

# Overturning of unreinforced masonry walls – predominant failure mechanism in historic masonry buildings

Authors:

[1]**Katarina Jajčević**, M.Sc. CE
katarina.jajcevic@grad.unizg.hr

[2]Assoc.Prof. **Marija Demšić**
marija.demsic@grad.unizg.hr

[2]Assoc.Prof. **Marta Šavor Novak**
marta.savor.novak@grad.unizg.hr

[2]Prof. **Josip Atalić**
josip.atalic@grad.unizg.hr

[2]Assoc.Prof.. **Mario Uroš**
mario.uros@grad.unizg.hr
**Corresponding author**

[1] University of Zagreb
Faculty of Civil Engineering
Croatian Center for Earthquake Engineering
[2] University of Zagreb
Faculty of Civil Engineering
Department of Technical Mechanics

Research Paper

Katarina Jajčević, Marija Demšić, Marta Šavor Novak, Josip Atalić, Mario Uroš

## Overturning of unreinforced masonry walls – predominant failure mechanism in historic masonry buildings

Masonry buildings, as the fundamental fabric of historic urban centers in Croatian cities, also represent the main source of damage during earthquakes. Analysis of the local failure mechanisms that caused this damage identifies in-plane and out-of-plane failure mechanisms. Out-of-plane mechanisms, besides significantly contributing to the damage caused by the December 29, 2020 earthquake in Petrinja, were rarely the focus of seismic performance of masonry buildings prior to the new generation of the HRN EN 1998 standard. The primary aim of this study is to demonstrate that the activation of such mechanisms poses a direct threat to human life and to emphasize the importance of developing skills for recognizing early signs of their formation and identifying structures prone to their activation. This is particularly relevant for field inspections following earthquakes, allowing timely assessment of the structural vulnerability of buildings and reducing risks to occupants and professionals. This study presents a categorization of out-of-plane failure mechanisms based on a methodology developed within this work for the historic core of Petrinja. The categorization is based on the geometric characteristics of documented mechanisms, their position within the building, and other relevant features, with the distribution of categories illustrated through pie charts and tables. Furthermore, a formulation of the out-of-plane wall behavior model is presented, first as a mathematical framework and then as a worked example in accordance with the guidelines of both the current and the new generation of the HRN EN 1998 standards.

**Key words:**
masonry buildings, historic urban centers, out-of-plane failure mechanisms, overturning, seismic vulnerability

Prethodno priopćenje

Katarina Jajčević, Marija Demšić, Marta Šavor Novak, Josip Atalić, Mario Uroš

## Prevrtanje nepridržanih zidova – prevladavajući mehanizam oštećenja starih zidanih zgrada

Tradicijske zidane zgrade, kao temeljno tkivo povijesnih jezgri hrvatskih gradova, predstavljaju kritičan čimbenik potresne oštetljivosti. Osnovne mehanizme oštećenja takvog zida možemo podijeliti na mehanizme otkazivanja u ravnini i izvan ravnine. Mehanizmi izvan ravnine, koji su znatno doprinijeli šteti tijekom potresa 29. prosinca 2020. u Petrinji, do nove generacije norme HRN EN 1998 rijetko su bili fokus analiza mehaničke otpornosti i stabilnosti tradicijskih zidanih zgrada. Bitan cilj ovog rada jest pokazati da aktiviranje takvih mehanizama predstavlja izravnu prijetnju ljudskim životima te istaknuti važnost razvijanja stručnih vještina za prepoznavanje ranih pokazatelja njihovog formiranja i identificiranja konstrukcija kod kojih je njihova aktivacija moguća. Posebno je ovo važno za terenske preglede nakon potresa kako bi se pravovremeno uočila ugroženost nosivog sustava građevine, ali i kako bi se adekvatno provela pojačanja ovog tipa građevina u potresnim područjima. U radu je napravljena kategorizacija mehanizama otkazivanja izvan ravnine koji su se dogodili na području povijesne jezgre Petrinje. Kategorizacija se temelji na geometrijskim karakteristikama dokumentiranih mehanizama, njihovom položaju unutar zgrade i drugim relevantnim značajkama. Također je prikazana formulacija modela ponašanja zidova opterećenih izvan svoje ravnine, na temelju čega je prikazan i proračunski primjer u skladu sa smjernicama postojećih i nove generacije normi HRN EN 1998.

**Ključne riječi:**
zidane zgrade, povijesna jezgra, mehanizmi otkazivanja izvan ravnine, prevrtanje, potresna oštetljivost

## 1. Introduction

Masonry buildings constitute a significant portion of the existing stock of residential and public buildings in Croatia, and it is particularly noteworthy that this building type has a long tradition and therefore often represents the majority of historic city centers as well as rural areas. A problematic aspect is that this type of building, in a large number of cases, often does not meet modern seismic requirements due to traditional construction methods, as buildings are usually constructed without adequate horizontal and vertical connectivity. Moreover, the devastating consequences of the Mw6.4 earthquake that struck the Petrinja and Sisak area on December 29, 2020, demonstrated that a major factor in the severe damage to local masonry buildings was the out-of-plane (OOP) wall failure mechanism [1]. This type of failure represents one of the most common and dangerous forms of mechanical instability in masonry buildings during earthquakes. Despite numerous studies based on experimental investigations [2-5], analytical [6, 7] and numerical models [8-14], predicting the activation of these damage mechanisms remains a subject of research and discussion due to the nonlinear interactions between walls, horizontal structural elements (roof and floor structures), and the influence of adjacent buildings. Considering that experimental models are generally very limited in terms of the geometry of the mechanism itself, and detailed numerical models based on discrete elements are extremely computationally and time demanding, identifying failure mechanisms [15] based on observations from previous earthquakes represents one of the fundamental pillars for understanding the seismic response of masonry buildings.

As a basis for the investigation of this type of damage in masonry buildings, photographic documentation from the database of the Croatian Center for Earthquake Engineering for the city of Petrinja was used [16, 17]. The damage database represents a valuable source of data for all studies of this event and the observed area. Within this study, OOP failure mechanisms observed in photographs and documented in inspection forms were analyzed, with particular attention given to their position within the building, geometric characteristics, and spatial orientation. The buildings in the observed area were further classified according to the potential for the development of out-of-plane failure mechanisms, which represents a notable contribution to this research, as it emphasizes the identification of the risk of their activation. As an additional result, some secondary characteristics of the building stock are presented, including the number of buildings damaged by the activation of out-of-plane failure mechanisms in neighboring buildings, the number of buildings removed after the earthquake, and the number of removed buildings in which the realization of this damage mechanism was observed.

In addition to the building classification, a more detailed analysis of local OOP mechanisms was also conducted. This analysis is performed using the kinematic theorem to determine the activation coefficient and the displacement capacity of the kinematic chain in the case of a nonlinear calculation. The seismic load is defined by the acceleration at the story level where the mechanism forms, considering the amplification effect associated with the building's fundamental vibration period. To further clarify the procedure, an example of a local OOP mechanism analysis is also presented in the study.

## 2. Overview of OOP mechanisms in Petrinja

### 2.1. Methodology for determining OOP mechanisms

Within this study, an analysis of OOP mechanisms occurred in the central area of Petrinja, caused by the series of earthquakes in December 2020, was conducted. Furthermore, considering the widespread typology of masonry buildings in the area, an assessment was also made regarding the potential occurrence of such mechanisms in the event of other earthquakes, based on the existing condition observed in rapid post-earthquake inspections of buildings. The research was carried out with the aim of reviewing and categorizing OOP mechanisms in the observed buildings, taking into account their geometry, direction of activation, occurrence of damage to the building caused by OOP mechanisms of adjacent buildings in a row, and the need for following demolition due to this type of damage. The studied area covers the historic streets of Petrinja, including Matija Gupca Street towards the southwest up to house number 105a, Ljudevit Gaj Street up to house number 57, and Artur Turkulin Street up to house number 49 towards northeast. Additionally, the entirety of Ivan Filipović Street, Ivan

**Figure 1. City plan of Petrinja and its surroundings, created by a group of students of the Military Mathematical School from Petrinja in 1821 [18]**

Gundulić Street, Vladimir Nazor Street, Josip Juraj Strossmayer Promenade, Stjepan Radić Square, and dr. Franjo Tuđman Square were considered, as well as Stjepan Radić Street up to house number 42 extending southwest. The total building stock within the studied area consists of 322 buildings. This area was selected because it follows the same streets along which, according to the earliest cartographic documentation shown in Figure 1, the urban fabric of present-day Petrinja began to develop. Figure 2 presents a mapped layout showing the buildings included in the analysis.

**Figure 2. Schematic map showing buildings selected for analysis**

The research was conducted based on the above-mentioned photographic documentation of damaged buildings from the database of the Croatian Centre for Earthquake Engineering [17], collected during rapid post-earthquake inspections in Petrinja, with the aim of identifying OOP mechanisms, determining the most frequent types of these failure mechanisms, and recognizing cracks indicating incipient formation or activation.

Building typologies that are most prone to local OOP mechanisms include structures built of unreinforced masonry. However, the risk of such failures also affects non-structural elements, such as chimneys and infill masonry that are not adequately anchored to load-bearing columns and beams, as well as brick façade elements, parapets and attic walls above the main cornice, and roof cornices [19]. Since engineering assessment of potential local mechanisms is largely based on experience from previous earthquakes [15, 9], an important objective of this research is to promote the development of skills for recognizing early signs of OOP mechanism formation, as well as identifying structures in which their activation is possible, particularly for engineers conducting field inspections, in order to ensure timely identification of threats to the building's load-bearing system.

A challenge that arises during rapid inspections, besides the time constraint implied by the term "rapid," which actually limits the amount of data collected, is the presence of hidden parts of the load-bearing structure beneath exterior walls and façade cladding, as well as the lack of documentation on building properties. For a number of buildings, this challenge was overcome by using images available from Google Street View from previous years [20], which show the load-bearing structure before the façade cladding was installed, or by photographs from the database taken in the building's attic space, where bare structural walls are visible. One of the peculiarities of buildings in the Petrinja area, regarding the classification of building typology based on the load-bearing system, is that in a significant number of cases the type of load-bearing structure is not uniform across storeys. A common example is that the ground floor or lower storeys are constructed as unreinforced masonry, while confined masonry appears in the attic. Part of this non-uniform structural system is the result of post-war reconstruction (repair of only damaged parts of the structure), but also of other subsequent interventions that were carried out selectively, with limited consideration of the existing structure. The non-uniformity of the load-bearing system presents a challenge when determining the potential occurrence of the observed type of mechanism, since on the lower storeys, which are more vulnerable in terms of load-bearing system type for this mechanism, the seismic excitation often has a very diverse frequency content, and the walls are loaded by the weight of the upper storeys, which generally has a stabilizing effect against the activation of OOP mechanisms. By contrast, in the attic such a mechanism is most often activated, because acceleration amplitudes increase with building height, and the response in the upper storeys is usually dominated by the first translational mode of building vibration. Nevertheless, its activation is not expected, given that the masonry is confined. Although resolving these uncertainties is not always straightforward, all buildings were ultimately systematized according to the criteria listed below, enabling a complete and consistent categorization of the examined buildings. Buildings for which no significant risk of OOP is determined are those constructed as reinforced concrete structures or as confined masonry structures.

In addition to classifying the observed damage into categories according to the activation of OOP mechanisms, it was also necessary to classify mechanisms that were fully developed, as well as those that were only potential, based on their form and position in the structure. Accordingly, the mechanisms were categorized into the following groups: *gable wall mechanism* (Figure 3), *façade wall mechanism* (Figure 4), and *mechanism of irregular geometry or atypical position* (Figure 5). An additional category consists of buildings in which OOP occurred, but the degree of collapse is such that the characteristics of the mechanisms cannot be reliably determined - these are buildings with damage state IV [21], which also included the formation of OOP mechanisms (Figure 6). For buildings in which multiple types of OOP occurred, the mechanism causing the greatest extent of damage was selected as the relevant one.

**Figure 3. Gable wall mechanism [17]**

Figure 4. Façade wall mechanism [17]

Figure 5. Mechanism of irregular geometry or atypical position [17]

Figure 6. Damage state IV (DS IV) with OOP mechanisms [17]

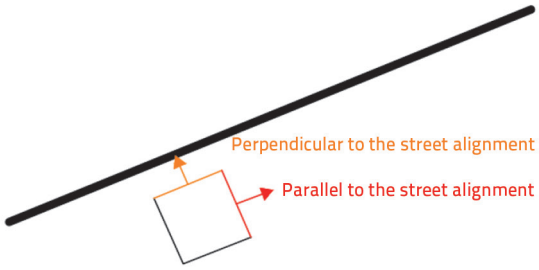


Figure 7. Directions of OOP mechanism failure

The next classification of mechanisms is based on the direction of their activation, whether fully developed or potential. The local direction is defined by the orientation of the mechanism relative to the street, while the global direction determines the general position of the mechanism in the environment. For clarification, the orientation of the gable wall mechanism is most often parallel to the street alignment, whereas the orientation of the façade wall mechanism is generally perpendicular to the street alignment (Figure 7).

Additionally, it was determined whether damage had occurred due to failure mechanisms in adjacent structures, and data on post-earthquake demolition were also processed, regardless of whether reconstruction was subsequently carried out or planned.

Based on all classifications conducted, the relevant results were selected, and the method of their presentation was defined. It is important to critically assess the results, which is why additional analyses were carried out to ensure that the structure of the observed sample of buildings does not influence the interpretation of the obtained results. For example, the predominant global orientation of a mechanism should not be considered individually but must also be examined in the context of the actual spatial arrangement of the dominant failure mechanism, e.g., the gable failure - the attic part of end wall.

For clarity, the methodology used to determine the characteristics of OOP mechanisms is presented in the flowchart in Figure 8.

## 2.2. Classification of damage associated with out-of-plane failure mechanisms

According to the research methodology described above, the buildings were classified into the following categories based on the OOP mechanism:

a) Fully developed OOP mechanism.
b) Cracks indicating formation of an OOP mechanism
c) Potential for OOP mechanism formation based on the building's material and construction method
d) No significant OOP risk based on the building's material and construction method

For the examined affected area, Figure 9.a shows the percentage distribution of the categories listed above, while Figure 9.b shows the distribution after excluding category (d), meaning buildings for which an OOP mechanism cannot occur were

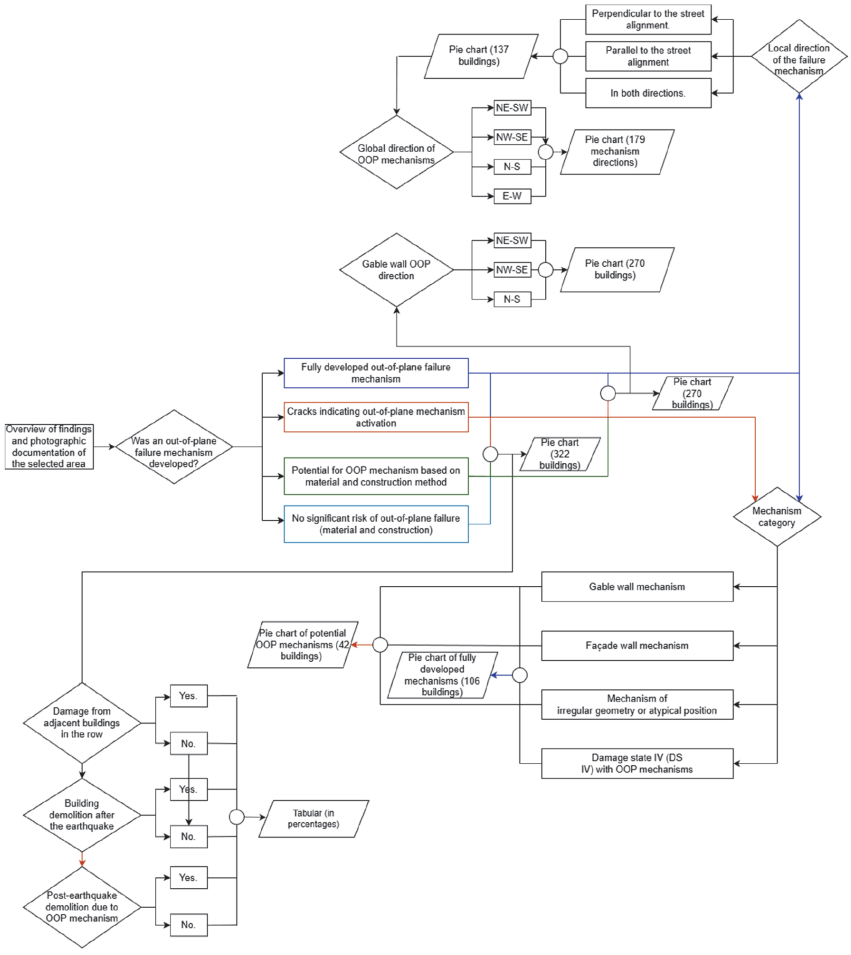


**Figure 8. Flow chart of the methodology [17]**

removed from the analysis. Therefore, Figure 9.a includes 322 buildings, while after excluding category (d), Figure 9.b presents the remaining 270 buildings.

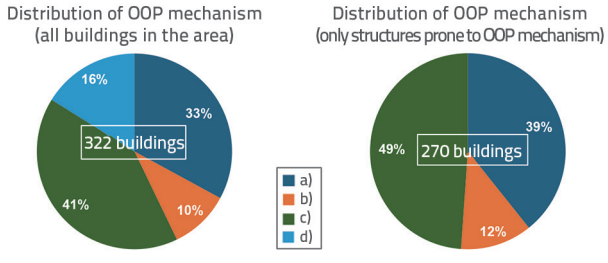


**Figure 9. Distribution of the studied buildings by category for: a) all buildings; b) only buildings where the occurrence of OOP mechanism is possible**

Buildings in which an OOP mechanism was activated were further organized according to their form and position, and were classified into the following categories already described in Section 2.1:

i) Gable wall mechanism
ii) Façade wall mechanism
iii) Mechanism of irregular geometry or atypical position
iv) Damage state IV (DS IV) with OOP mechanisms

A visual representation of the distribution of buildings according to these categories, which provides better insight into their prevalence, is shown in Figure 10. The number of 106 buildings represents 33 % of the total 322 buildings shown in Figure 9.a. For buildings where cracks indicating activation of an OOP mechanism were observed, Figure 11 shows that the gable wall mechanism is again the most prevalent. This is expected, given that attic walls of gable walls are typically unrestrained elements. The total of 42 buildings corresponds to ~ 10 % of the 322 buildings shown in Figure 9.a, with an additional 11 buildings included in which, besides developed OOP mechanisms, cracks indicating activation of these mechanisms were also observed. It is also important to note that 12 % of the recorded damage relates to a potential facade wall mechanism, indicating a significant level of seismic vulnerability of these elements, which commonly support timber floor structures. Further analysis of the local failure direction of developed OOP mechanisms, their orientation relative to the street alignment, is presented in Figure 12.

The largest share corresponds to mechanisms whose activation direction is parallel to the street, which largely reflects the typical orientation of gable walls. In a considerable portion of the damaged buildings, amounting to 31 %, local mechanisms were activated in both directions. The smallest share in this case corresponds to mechanisms oriented perpendicular to the street, which can in most cases be associated with the activation of facade wall mechanisms.

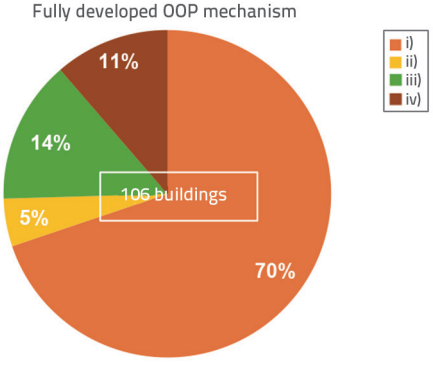


**Figure 10. Categorized distribution of OOP mechanisms**

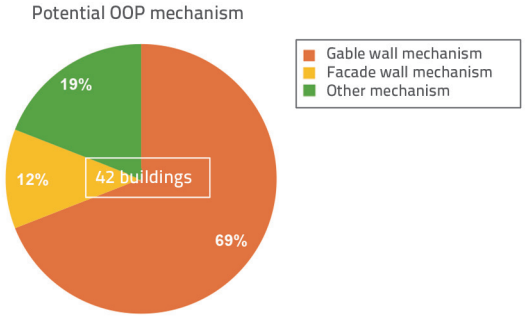


**Figure 11. Categorized distribution of potential OOP mechanisms**

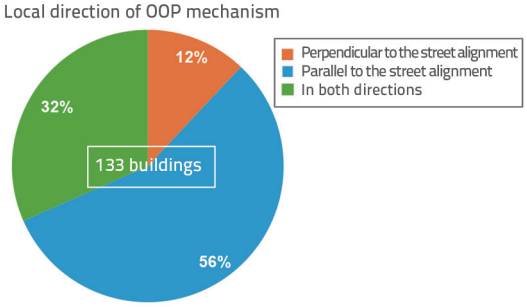


**Figure 12. Distribution of OOP mechanisms by orientation relative to the street alignment**

A further observation concerns the global orientation of OOP mechanisms, illustrated in Figure 13.a, while Figure 13.b shows the expected global orientation of the predominant mechanism.

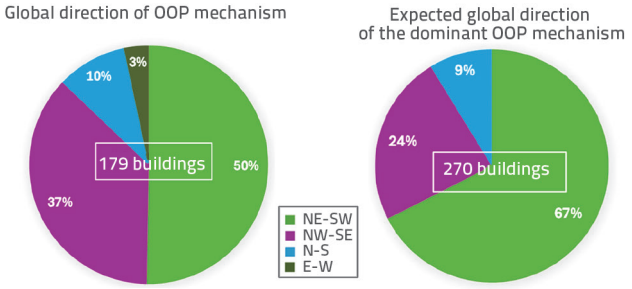


**Figure 13. Global orientation of a) developed or activated OOP mechanism; b) predominant OOP mechanism**

Figure 13.a presents a total of 179 mechanism directions derived from 137 buildings in which an OOP failure mechanism was either developed or indicated by cracks suggesting its activation, with an additional 42 directions corresponding to buildings where the mechanism developed in both directions. The expected global orientation refers to the position of the gable wall in all buildings where an OOP mechanism was either developed, indicated by cracks suggesting activation, or could potentially be activated due to the building's material and construction method. Consequently, the number of buildings shown in Figure 13.b, 270 - corresponds to the number of buildings considered in Figure 9.b. The two figures are presented side by side to allow direct comparison. The predominance of the NE–SW global orientation reflects the orientation of the most common mechanism type, namely the gable wall mechanism. This result follows from the orientation of the surveyed buildings and is consistent with the alignment of the streets along which they are arranged.

For clarity, the results of additional analyses conducted on the entire dataset of 322 examined and analyzed buildings are presented in Table 1. These results provide insight into the percentage of buildings damaged due to the activation of OOP mechanisms in adjacent buildings within a row, the proportion of buildings demolished after the earthquake, as well as changes in this proportion when considering only buildings with developed OOP mechanisms.

**Table 1. Impact on surrounding buildings and demolition of damaged buildings**

| Analysis of the considered buildings | Yes [%] | No [%] |
|---|---|---|
| Damage to buildings caused by the OOP mechanism of a neighboring building | 14 | 86 |
| Building demolished after the earthquake | 27 | 73 |
| Building demolished after the earthquake due to OOP damage | 48 | 52 |

Figure 14 presents a map showing the epicenter and peak ground acceleration contours obtained from the website of the United States Geological Survey (USGS) [22]. The peak ground acceleration contours were scaled (proportionally intensified) to ensure visibility in Figure 15, which again shows the map of the selected study area. In Figure 15, the planes in which an OOP mechanism was developed or cracks indicating activation of the mechanism were observed are marked for each building. In addition, the buildings are hatched according to the OOP mechanism category.

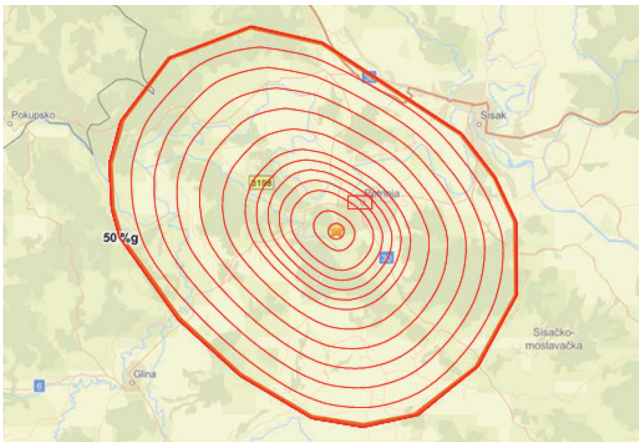


**Figure 14. Epicenter and peak ground acceleration contours in relation to the location of Petrinja [22]**

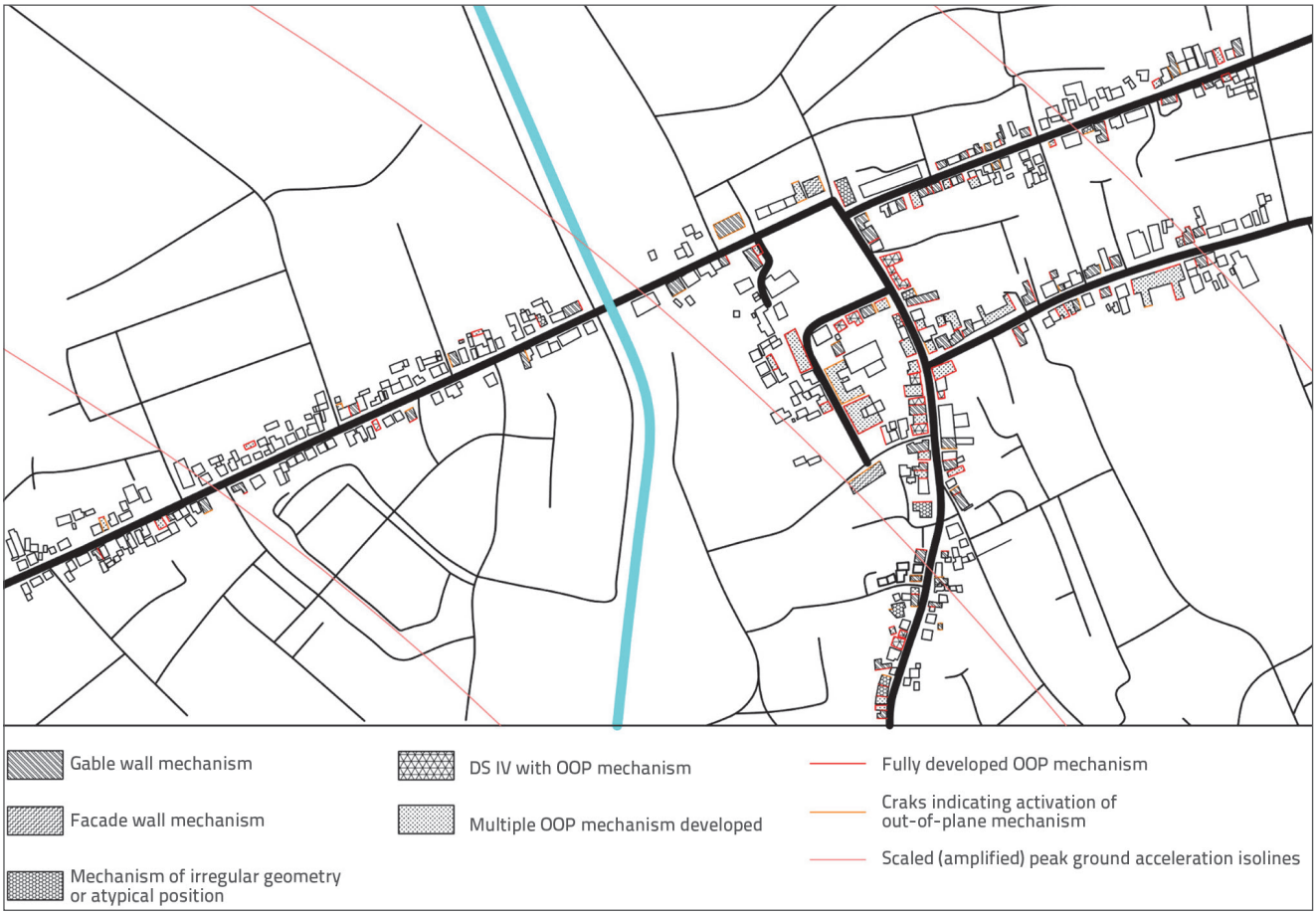


**Figure 15. Map of the selected area with the analyzed data**

## 3. Formulation of the out-of-plane behavior model of a wall

### 3.1. Mathematical model of local out-of-plane mechanism

The assessment of the seismic resistance against overturning of masonry walls is based on the equilibrium condition of all actions that produce stabilizing and destabilizing overturning moments. This fundamental principle of equilibrium defines the activation state of the mechanism, assuming the formation of line hinges around which rigid bodies rotate (Figure 16). For this equilibrium condition, kinematic analysis based on the principle of virtual work is most commonly used. This procedure determines the required horizontal force, or the corresponding acceleration, needed to activate the mechanism into motion, considering the inertial effects of the masses and the geometry of the elements in the kinematic chain.

The procedure begins with defining, or identifying, the type of local mechanism that could form, i.e., its geometric parameters and constraints (hinges and supports). This is a crucial step because it directly affects the kinematically admissible displacement field. Next, all loads, horizontal and vertical forces, acting on the individual wall segments must be applied to formulate the equation of virtual work:

$$\alpha_0 = \left(\sum P_i \delta_{x,i} + \sum P_j \delta_{x,j}\right) - \sum P_i \delta_{y,i} - \sum F_h \delta_h = L_f \qquad (1)$$

where $P_i$ represents all the weights acting directly on the wall segments that generate inertial forces, while $P_j$ denotes the general weights that do not act directly on the blocks, but whose inertial effects are transferred to the mechanism because they cannot be effectively transferred to other load-bearing elements. In addition to gravitational forces, other forces acting on the blocks $F_h$ must be considered, which may have a destabilizing effect (e.g., thrust from vaults) or a stabilizing effect (e.g., friction forces at the junction with adjacent walls) on the mechanism itself. The value $L_f$ includes the total work of the internal forces of the mechanism (e.g., sliding with friction between the mechanism blocks (wall segments) or connected flexible floor structures, and similar effects).

By solving the equation, the coefficient $\alpha_0$ is determined, which defines the peak value of the horizontal actions that cause the mechanism to start moving (activation) - this state of the mechanism can be associated with a state of limited damage. In the case of performing a nonlinear kinematic procedure, it is necessary to determine the coefficient $\alpha$ not only for the initial configuration of the kinematic chain, but also for subsequent configurations describing the positions of the mechanism during motion, which are described by the horizontal displacement $d_c$

of a selected control point. In general, the value of $\alpha$ gradually decreases until it vanishes at the displacement $d_0$. The $\alpha$-d curve obtained from the nonlinear kinematic analysis describes the force-displacement capacity of the considered local mechanism (or the $\alpha$-d curve describes the capacity of the local mechanism in terms of the relationship between the horizontal action and the corresponding displacement).

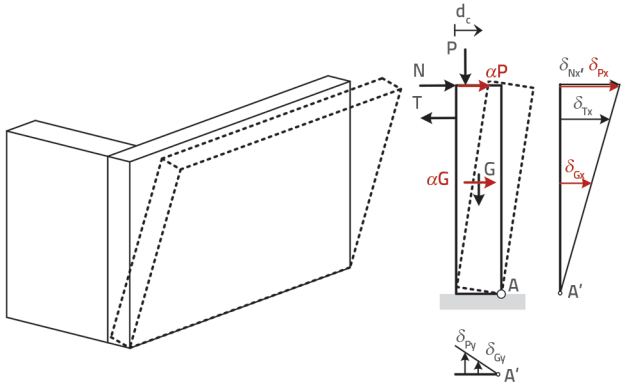


**Figure 16. Initial and displaced configuration of the overturning mechanism, showing the virtual displacement field**

When the permanent and variable actions remain constant during the development of the mechanism, the curve $\alpha(d_c)$ can be described as linear up to the displacement $d = d_{c0}$, as shown in Figure 17. The value of the ultimate displacement $d_{C0}$ corresponds to the position of the mechanism for which $\alpha = 0$, i.e., the position of unstable equilibrium in which the mechanism completely loses stability. If the loads change during the development of the mechanism, it is necessary to successively determine this capacity curve based on the equilibrium condition at each step.

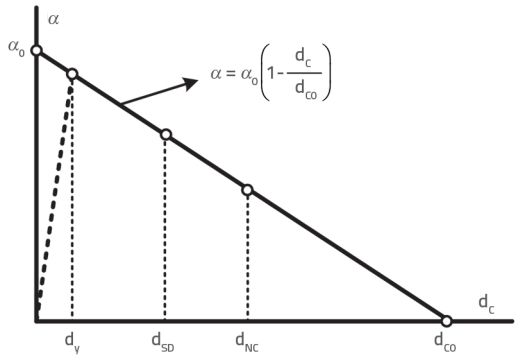


**Figure 17. Capacity curve of a simple block overturning mechanism**

The acceleration and displacement values determined for such a simplified kinematic system must satisfy safety requirements. Accurately assessing the influence of acceleration amplification due to the response of the global structure requires an analysis of the primary (main structure) and secondary (local mechanism) systems, taking their interaction into account, using complex performance models. On the other hand, the approach based on the Floor Response Spectrum neglects the dynamic interaction between the primary and secondary systems and is based on determining the floor spectrum, which accounts for the filtering effect of acceleration at higher stories of the structure.

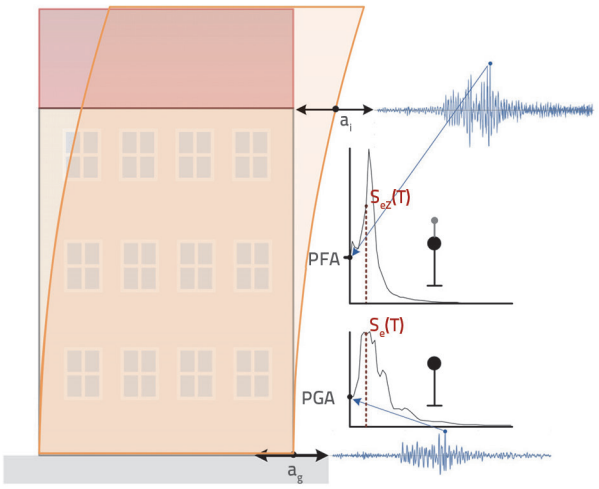


**Figure 18. Acceleration amplification caused by the filtering effect and the floor response spectrum**

If we assume that the ground acceleration is described by the time function $a_g(t)$, from which a response spectrum can be formed $S_e(T)$, then for a given damping ratio we obtain the conventional response spectrum. For a period $T$ = 0, the spectrum value corresponds to the peak ground acceleration (PGA). Under the dynamic excitation, the structure develops its own dynamic response. In a simplified formulation, the total acceleration at a given height of the structure can be described by the time function $a_i(t)$, which represents the acceleration of story $i$. If time integration procedure is carried out for this input function for a given damping value, it is possible to form the response spectrum, thus obtaining the so-called floor response spectrum. This spectrum includes the filtering effects of the base acceleration record that arise due to the dynamic response of the structure. The peak floor acceleration (PFA) corresponds to the spectrum value at $T$ = 0, i.e., for an ideally rigid sub-system, while the pseudo-acceleration for an elastic sub-system with period $T$ corresponds to the value $S_e(T)$ if it is primarily influenced by ground motion, or to $S_{eZ}(T)$ if it is located at height and is predominantly influenced by the structural response. The shape and magnitude of the floor response spectrum are influenced by the fundamental dynamic characteristics of the structure (mass, stiffness, damping), as well as possible nonlinearities during the response. It is important to emphasize that when the structure enters the nonlinear range, the acceleration amplification effects generally decrease, while at the same time changes occur in the region of peak values [8, 9, 13, 23]. This is a consequence of the fact that nonlinear response changes the fundamental dynamic parameters of the system.

Since the determination of the floor response spectrum requires performing a dynamic analysis of the structure, various formulations have been proposed in the literature that enable the direct formation of the floor response spectrum. An

overview of these approaches is given in [8]. It is important to emphasize, as confirmed by numerous studies, that the initial period of the secondary system can have a significant influence on the estimation of acceleration demands. In this study, the analysis is limited to the effects of acceleration amplification as recommended in Eurocode 8 (HRN EN 1998 [24, 25]). The currently valid standard considers the effects of acceleration amplification only for non-structural elements:

$$S_{a,Z} = a_g S \left[ \frac{3\left(1+\frac{Z}{H}\right)}{1+\left(1-\frac{T}{T_1}\right)} - 0,5 \right] \quad (2)$$

where Z is the height at which the element is located, while the periods $T_1$ and $T$ refer to the periods of the main structure and the non-structural element, respectively. For the assessment of the action effect, the importance factor and the behavior factor of the element are taken into account. On the other hand, according to the proposal of the new generation of the standard, it will be necessary for existing structures to verify the local out-of-plane mechanisms (OOP) in masonry buildings in cases where the models used do not include this type of damage. In a simplified analytical approach, assuming rigid elements, the seismic demand imposed on the element can be determined according to the following expression:

$$\max\left( S_e, S_{eZ} = \Gamma_1 \frac{Z}{H} S_e(T_1) \right) \quad (3)$$

These expressions in their original formulation also use selected safety factors and behavior factors. For the assessment of the seismic demand of a local mechanism, its response must be reduced to an equivalent single-degree-of-freedom (SDOF) system, described by the corresponding values of acceleration (or force) and displacement. In doing so, the conversion coefficient $\Gamma$ is used to link the behavior of the local mechanism with the idealized equivalent system:

$$\Gamma_1 = \frac{\sum P_i \delta_{x,i}}{\sum P_i \delta_{x,i}^2} \quad (4)$$

The theoretical framework presented above, and the corresponding expressions provide the basis for quantifying seismic demands on structural elements with respect to acceleration amplification effects, in accordance with the current provisions and the guidelines of the new generation of the EN 1998-3 standard [26, 27]. Since the newly proposed code approaches are still in the process of evaluation and adaptation at national levels, a worked example within a simplified analytical model will be presented below.

## 3.2 Case studies of OOP mechanisms

In this chapter, the assessment of the top-story façade wall and the gable wall parapet of the building shown in Figure 19 is performed. It is assumed that OOP mechanisms in both walls occur by overturning, i.e., each wall is modeled as a rigid block that rotates around a line hinge. The position of the line hinge is located at a height of 7 m, while the total height of the building is approximately 9.5 m. The dimensions and the kinematic model of the first wall under consideration are shown in Figure 20, together with the prescribed displacement field used for the calculation of virtual work within the linear kinematic analysis. The z and y components of the center of gravity, as well as the values of the self-weight and additional permanent load, are determined. The horizontal and vertical displacements of the forces are obtained as functions of the rotation angle $\delta\varphi$, and the activation coefficient of the mechanism $\alpha$ is derived using the virtual work equation.

Additional parameters that are ultimately required for the verification of damage limit states are the modal mass $m^*$, the modal participation factor $\Gamma_1$ and the conversion factor $\Gamma$. The kinematic model used in the nonlinear kinematic analysis, i.e., in the displacement capacity analysis, is shown in Figure 21 together with the indicated displacement configuration. The result of the nonlinear kinematic analysis is the equivalent spectral displacement , which is later used for the verifications of individual damage limit states.

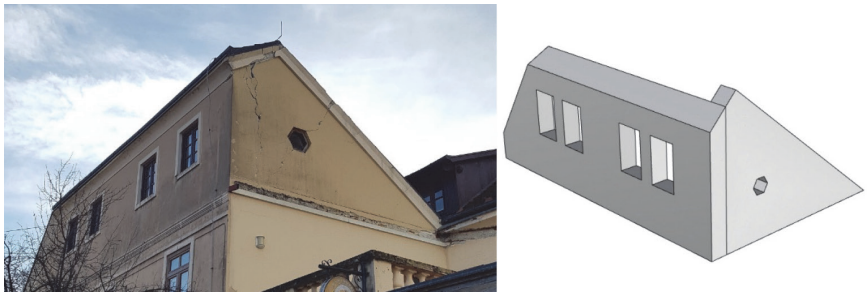

**Figure 19. Geometry of the local out-of-plane mechanism**

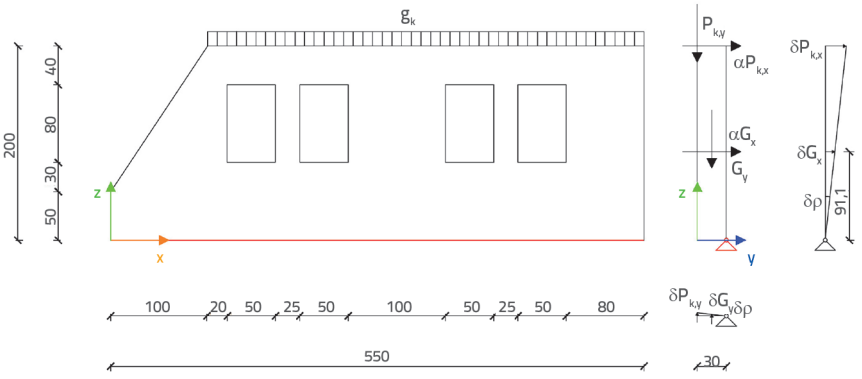


**Figure 20. Dimensions and kinematic model of the wall being considered**

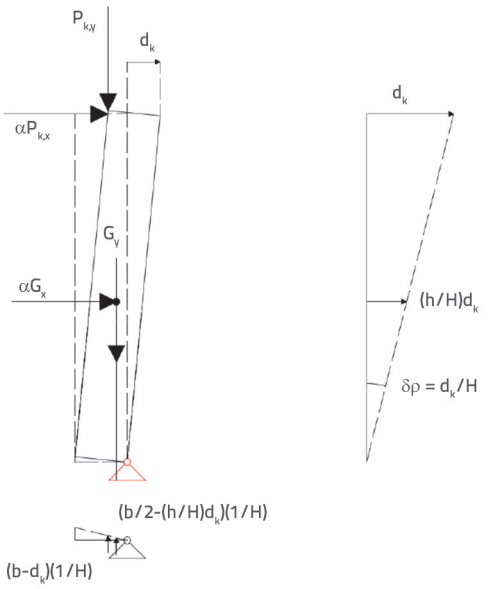


**Figure 21. Displacement configuration in nonlinear kinematic analysis**

As already mentioned, the current standard HRN EN 1998 [24, 25] only provides guidelines for the verification of non-structural elements, so a more elaborated approach has mainly relied on the Italian guidelines [28, 29], since their building typology is most similar to ours. However, the new generation of Eurocode 1998-3 [26, 27] introduces a more systematic assessment through the application of linear and nonlinear analyses and the verification of damage limit states at three levels: Damage Limitation (DL), Significant Damage (SD), and Near Collapse (NC). Table 2 presents the calculation results for the first wall under consideration, from which it is evident that the analysis does not satisfy, i.e., the OOP mechanism is activated, according to the existing standard HRN EN 1998 [24, 25] if the wall is considered as a non-structural element. In contrast, in the verifications performed according to the proposal of the new generation of that standard [26, 27], the analysis does not satisfy the Damage Limitation (DL) and Significant Damage (SD) limit states, while it satisfies the Near Collapse (NC) limit state. The return period used in the analysis should be selected according to the corresponding limit state. However, due to the current lack of data, a return period of $T_p = 475$ years was used for all limit states, which is typically used for the SD (Significant Damage) state. Additionally, Figure 22 graphically shows the development of the capacity curve $F^*$ - $d^*$ for the case under consideration, and the criteria for the verification of limit states according to the corresponding displacement are visually indicated.

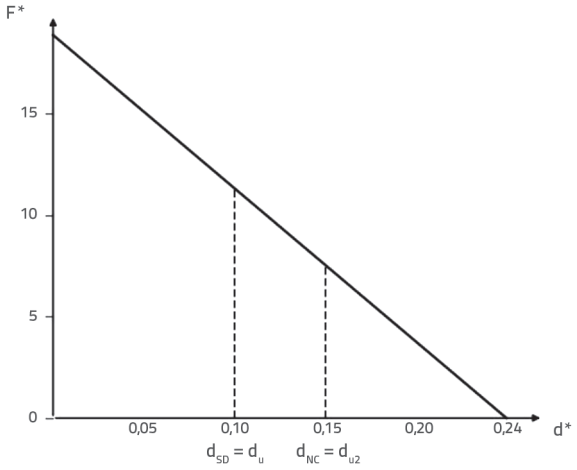


**Figure 22. Capacity curve of the first examined wall**

**Table 2. Calculation results for the first example**

| Analysis | | | | Verification for damage states | | | |
|---|---|---|---|---|---|---|---|
| **Linear kinematic analysis** | | | | **HRN EN 1998-3:2011 - Non-structural elements** | | | |
| Center of gravity | $z_T$ | 0,911 | [m] | Floor acceleration coefficient | $S_{a,Z}$ | 0,261 | |
| | $y_T$ | 0,15 | [m] | Horizontal seismic force | $F_a$ | 17,98 | [kN] |
| Self-weight | G | 45,88 | [kN] | $M_{stabilizing} > M_{overturning}$ | | | |
| Roof thrust | $g_{strop}$ | 7 | [kN/m'] | 16,332<16,36 → activation of the collapse mechanism | | | |
| | $P_k$ | 31,5 | [kN] | **HRN EN 1998-3:2025** | | | |
| Displacement values | $\delta_{G,x}$ | 0,911 | [δφ] | **DL (DAMAGE LIMITATION)** | | | |
| | $\delta_{G,y}$ | 0,15 | [δφ] | Resistance of the DL state as the equivalent system force | $F_{DL}$* | 18,89 | [kN] |
| | $\delta_{Pk,x}$ | 2 | [δφ] | $M_{stabilizing} > M_{overturning}$ | | | |
| | $\delta_{P,y}$ | 0,3 | [δφ] | 16,332<17,21 → does not satisfy | | | |
| Activation coefficient | α | 0,156 | | **SD (SIGNIFICANT DAMAGE)** | | | |
| Effective modal mass | m* | 6,28 | [t] | Equivalent system displacement for SD state | $d_{SD}=d_u$ | 0,098 | [m] |
| Modal participation factor | $\Gamma_1$ | 1,286 | | Linear equivalent period for SD state | $T_{SD}$ | 1,171 | [s] |
| Transformation factor | Γ | 0,639 | | $\gamma_{Sd} S_{eZ}(T_{SD}) \left(\frac{T_{SD}}{2\pi}\right)^2 \leq \frac{d_{SD}}{\gamma_{Rd}}$ | 0,09 > 0,06 → *does not satisfy* | | |
| **Nonlinear kinematic analysis** | | | | | | | |
| Control displacement | $d_k$ | 1 | | **NC (NEAR COLLAPSE)** | | | |
| Virtual displacements | $\delta_{G,y}$ | 0,075-0,228·$d_k$ | | Equivalent system displacement for NC state | $d_{NC}=d_{u2}$ | 0,147 | [m] |
| | $\delta_{P,k,y}$ | 0,15-0,5·$d_k$ | | Linear equivalent period for NC state | $T_{NC}$ | 1,757 | [s] |
| | $\delta_{G,x}$ | 0,228·$d_k$ | | $\gamma_{Sd} S_{eZ}(T_{NC}) \left(\frac{T_{NC}}{2\pi}\right)^2 \leq \frac{d_{NC}}{\gamma_{Rd}}$ | 0,05 ≤ 0,09 → *does not satisfy* | | |
| | $\delta_{P,k,x}$ | 0,5·$d_k$ | | | | | |
| | $d_{k,0}$ | 0,312 | | Partial factor for actions | $\gamma_{Sd}$ | 1,15 | |
| Equivalent spectral displacement | d* | 0,245 | [m] | Partial factor for resistance | $\gamma_{Rd}$ | 1,7 | |

**Table 3. Calculation results for the second example**

| Analysis | | | | Verification for damage states | | | |
|---|---|---|---|---|---|---|---|
| **Linear kinematic analysis** | | | | **HRN EN 1998-3:2011 - Non-structural elements** | | | |
| Center of gravity | $z_T$ | 0,859 | [m] | Floor acceleration coefficient | $S_{a,Z}$ | 0,261 | |
| | $y_T$ | 0,15 | [m] | Horizontal seismic force | $F_a$ | 16,79 | [kN] |
| Self-weight | G | 42,88 | [kN] | $M_{stabilizing} > M_{overturning}$ | | | |
| Roof thrust | $\delta_{G,x}$ | 0,859 | [δφ] | 6,43<14,42 → does not satisfy | | | |
| | $\delta_{G,y}$ | 0,15 | [δφ] | **HRN EN 1998-3:2025** | | | |
| Activation coefficient | α | 0,174 | | **DL (DAMAGE LIMITATION)** | | | |
| Effective modal mass | m* | 4,68 | [t] | Resistance of the DL state as the equivalent system force | $F_{DL}$* | 6,41 | [kN] |
| Modal participation factor | $\Gamma_1$ | 1,286 | | $M_{stabilizing} > M_{overturning}$ | | | |
| Transformation factor | Γ | 1,164 | | 6,432>5,501 → does satisfy | | | |
| **Nonlinear kinematic analysis** | | | | **SD (SIGNIFICANT DAMAGE)** | | | |
| Control displacement | $d_k$ | 1 | | Equivalent system displacement for SD state | $d_{SD}=d_u$ | 0,06 | [m] |
| Virtual displacements | $\delta_{G,y}$ | 0,06-0,138·$d_k$ | | Linear equivalent period for SD state | $T_{SD}$ | 0,859 | [s] |
| | $\delta_{G,x}$ | 0,228·$d_k$ | | $\gamma_{Sd} S_{eZ}(T_{SD}) \left(\frac{T_{SD}}{2\pi}\right)^2 \leq \frac{d_{SD}}{\gamma_{Rd}}$ | $0,084 < 0,141 \rightarrow does\ satisfy$ | | |
| | $d_{k,0}$ | 0,435 | | | | | |
| Equivalent spectral displacement | d* | 0,06 | [m] | | | | |

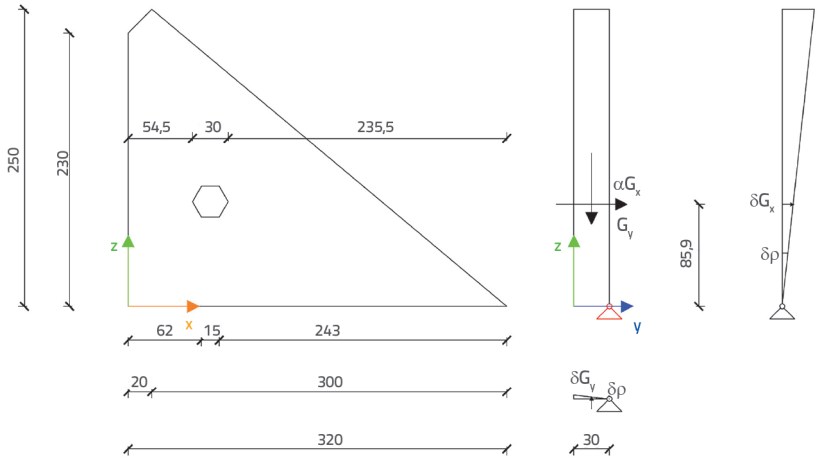


**Figure 23. Dimensions and kinematic model of the wall being considered**

The same procedure was also carried out for the calculation of the transversal wall, for which only self-weight was considered. Since the analyses satisfy the requirements for the damage limitation (DL) and significant damage (SD) limit states, the analysis for the near-collapse (NC) state was not performed. As in the previous example, Figures 23 and 24 show, respectively, the dimensions and the kinematic model of the wall under consideration, and the kinematic model used in the nonlinear analysis. The results of the calculations are presented in Table 3, while Figure 25 shows the corresponding development of the capacity curve *F* - d**.

The results indicate that the first wall is more vulnerable in the case of OOP, as it does not satisfy the requirements even when checked according to the current regulations for non-structural elements [24, 25], nor according to the future regulations [26, 27], up to the near-collapse (NC) state. However, this does not mean that the second investigated wall can be neglected. It does not comply with the current regulation when considered as a non-structural element, and the observed cracks indicate possible in-plane damage to the wall.

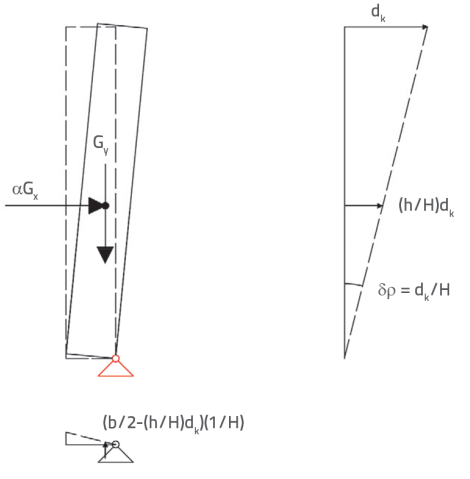


**Figure 24. Displacement configuration in nonlinear kinematic analysis**

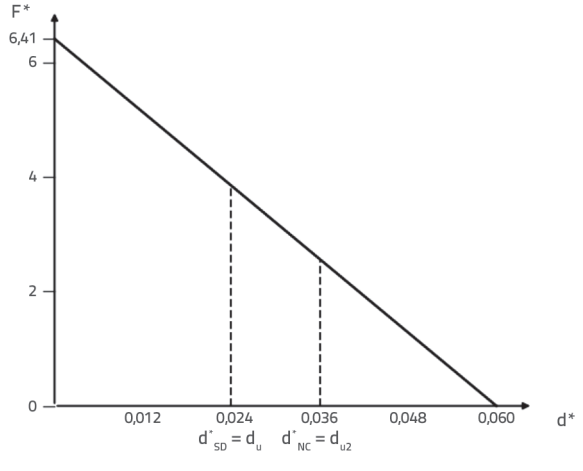


**Figure 25. Capacity curve of the second examined wall**

## 4. Conclusion

The methodology addressed in this paper was applied to a sample of 322 buildings, selected based on historical maps with the aim of including the oldest structures and the highest proportion of buildings constructed as unreinforced masonry. The results of the first analysis of methodology, i.e., the distribution of buildings according to the potential activation of the OOP mechanism, show that 270 out of 322 buildings are susceptible to this type of failure. This confirms that the sample is relevant and representative, and that it is characteristic of the typologies of historic urban cores in Croatia in many cases. The analysis also shows that, based on data collected during rapid post-earthquake surveys, it is possible to identify buildings susceptible to activation of such a mechanism, which can serve as a guideline for further actions regarding these buildings. An important outcome of this research is the share of buildings in which the OOP mechanism occurred-106 buildings (33 %)-and the number of buildings where cracks indicating its activation were observed-32 buildings (10 %).

The buildings were then classified into categories according to the location and geometric characteristics of the mechanisms in order to determine which mechanism category is most prevalent. In this sample, the most common mechanisms were, as expected, those related to gable walls. Considering the identified most frequent mechanism category, the results of the categorization of realized failure mechanisms-according to the direction of failure, locally relative to the street alignment, and globally relative to the cardinal orientation-are presented in parallel with the expected global failure direction of the most common mechanism category for all buildings susceptible to OOP (270 buildings). This parallel presentation is necessary to avoid the misleading conclusion that certain global failure directions are more frequent because the mechanisms are more prone to activation in those directions, whereas the most common mechanism is simply oriented according to the street alignment in the sample studied. When this is considered together with the map showing the axes of the buildings where OOP occurred, the only conclusion that can be drawn is that the positions of the gable walls in the studied sample are extremely unfavorably located in space relative to the scaled isoseismal lines of peak ground acceleration, i.e., relative to the epicenter.

Additional analyses show that a significant share of buildings, 14 % (46 buildings), exhibited damage caused by OOP of adjacent buildings in a row. This highlights that in historic urban cores, where buildings are typically constructed in continuous blocks and rows, OOP mechanisms pose a risk not only to the building in which they develop but also to the adjacent, lower buildings.

Another notable finding is that 27 % of the studied buildings were demolished after the earthquake, a total of 85 buildings. Considering only the buildings where the OOP mechanism was activated, this share rises to 48 %, i.e., 51 out of 106 buildings, confirming that this is the predominant damage mechanism for old masonry buildings.

This methodology provides a solid basis for studying OOP mechanisms characteristic of the building typologies in historic urban centers of continental Croatia, which may be a relevant factor in assessing seismic risk in these areas. Furthermore, considering the earthquakes that occurred, an additional component of the research would be to determine the sequence of events, i.e., whether the OOP mechanism occurred after in-plane damage of the elements, since there is limited data on damage from the previous Mw 5.2 earthquake on 28 December 2020. Taking this into account, the analysis of local in-plane failure mechanisms could enable a more comprehensive assessment of damage in the studied area, and it would be desirable to extend the sample to the entire town of Petrinja. Since the research is based on the observed state and post-earthquake surveys, it would also be useful to include the stock of restored buildings to obtain an updated risk assessment of potential OOP mechanism activation.

## Acknowledgements

The authors would like to express their sincere gratitude to the Croatian Centre for Earthquake Engineering-Intervention Service for providing access to the photo database, as well as to all engineers who contributed to its development. The authors also acknowledge the financial support provided by the Croatian Science Foundation (UIP-2020-02-1128) and the Croatian Centre for Earthquake Engineering (A679117 HPC).

## REFERENCES

[1] Atalić, J., Demšić, M., Baniček, M. Uroš, M., Dasović, I., Prevolnik, S., Kadić, A., Šavor Novak, M., Nastev, M.: The December 2020 magnitude (Mw) 6.4 Petrinja earthquake, Croatia: seismological aspects, emergency response and impacts, Bulletin of Earthquake Engineering, 21 (2023), pp. 5767–5808, https://doi.org/10.1007/s10518-023-01758-z

[2] Costa, A.A., Arêde, A., Costa, A., Oliveira, C.S.: Out-of-plane behaviour of existing stone masonry buildings: Experimental evaluation, Bulletin of Earthquake Engineering, 10 (2012), pp. 93-111, https://doi.org/10.1007/s10518-011-9332-9

[3] Costa, A.A., Arêde, A., Campos Costa, A., Penna, A., Costa, A.: Out-of-plane behaviour of a full-scale stone masonry façade, Part 1: specimen and ground motion selection, Earthquake Engineering & Structural Dynamics, 42 (2013), pp. 2087–2095, https://doi.org/10.1002/eqe.2313

[4] Costa, A.A., Arêde, A., Campos Costa, A., Penna, A., Costa, A.: Out-of-plane behaviour of a full scale stone masonry façade, Part 2: Shaking table tests, Earthquake Engineering & Structural Dynamics, 42 (2013), pp. 2097–2111, https://doi.org/10.1002/eqe.2314

[5] Ferreira, T.M., Costa, A.A., Arêde, A., Gomes, A., Costa, A.: Experimental characterization of the out-of-plane performance of regular stone masonry walls, including test setups and axial load influence, Bulletin of Earthquake Engineering, 13 (2015), pp. 2667-2692, https://doi.org/10.1007/s10518-015-9742-1

[6] Lagomarsino, S.: Seismic assessment of rocking masonry structures. Bulletin of Earthquake Engineering, 13 (2015), pp. 97–128, https://doi.org/10.1007/s10518-014-9609-x

[7] Doherty, K.: An Investigation of the weak link in the seismic load path of unreinforced masonry buildings, PhD Thesis, Adelaide University, Department of Civil and Environmental Engineering, 2000.

[8] Degli Abbati, S., Cattari, S., Lagomarsino, S.: Theoretically-based and practice-oriented formulations for the floor spectra evaluation, Earthquakes and Structures, 15 (2018) 5, pp. 565-581, https://doi.org/10.12989/eas.2018.15.5.565

[9] Degli Abbati, S., Cattari, S., Lagomarsino, S.: Validation of a practice-oriented floor spectra formulation through actual data from the 2016/2017 Central Italy earthquake. Bulletin of Earthquake Engineering, 20 (2022), pp. 7477-7511, https://doi.org/10.1007/s10518-022-01498-6

[10] Grillanda, N., Valente, M., Milani, G.: ANUB-Aggregates: a fully automatic NURBS-based software for advanced local failure analyses of historical masonry aggregates, Bulletin of Earthquake Engineering, 18 (2020) 8, pp. 3935-3961.

[11] Chiozzi, A., Grillanda, N., Milani, G., Tralli, A.: UB-ALMANAC: An adaptive limit analysis NURBS-based program for the automatic assessment of partial failure mechanisms in masonry churches, Engineering Failure Analysis, 85 (2018), pp. 201–220.

[12] Lestuzzi, P.:Simplified out-of-plane seismic behavior assessment of non-structural rocking walls, Frontiers in Built Environment, 9 (2023), 10.3389/fbuil.2023.1113847.

[13] Pinasco, S., Demšić, M., Pilipović, A., Šavor Novak, M., Uroš, M., Lagomarsino S., Cattari S.: Seismic fragility assessment of existing masonry buildings in aggregate located in Zagreb, Bull Earthquake Eng, 23 (2025), pp. 2715–2741, https://doi.org/10.1007/s10518-025-02156-3

[14] Vanin, F., Penna, A., Beyer, K.: A three-dimensional macroelement for modelling the in-plane and out-of-plane response of masonry walls. Earthquake Engineering & Structural Dynamics, 49 (2020) 12, pp. 1365–1389, https://doi.org/10.1002/eqe.3277

[15] D'Ayala D, Speranza E.: Definition of Collapse Mechanisms and Seismic Vulnerability of Historic Masonry Buildings. Earthquake Spectra, 19 (2003) 3, pp. 479-509, https://doi.org/10.1193/1.1599896

[16] Atalić, J.; Uroš, M.; Šavor Novak, M.; Demšić, M.; Baniček, M.; Kadić, A.; Oreb, J.: The Croatian Centre for Earthquake Engineering: establishment, activities and future opportunities. Proceedings of the Third European Conference on Earthquake Engineering and Seismology – 3ECEES. Arion, Cristian; Scupin, Alexandra; Țigănescu, Alexandru (ur.). Bukurešt, CONSPRESS, pp. 2088-2097, 2022.

[17] HCPI: Building usability database, Croatian Center for Earthquake Engineering, Faculty of Civil Engineering, University of Zagreb. (2020).

[18] Lipovac, N.: Petrinja, Prostorno-povijesni razvoj grada očitan sa starih grafika, planova i karata, Arhitektonski fakultet Sveučilišta u Zagrebu, Zagreb, 2010.

[19] Potresno inženjerstvo - Obnova zidanih zgrada, Uroš, M., Todorić, M., Crnogorac, M., Atalić, J., Šavor Novak, M., & Lakušić, S. (ur.). Zagreb: Sveučilište u Zagrebu, Građevinski fakultet. ISBN: 978-953-8168-43-7, 2021.

[20] Google: Google Street View imagery of Petrinja, Croatia, 2011, 2012, 2018, dostupno na: https://www.google.com/streetview, pristupljeno 10. 10. 2025.

[21] Uroš, M., Šavor Novak, M., Atalić, J., Sigmund, Z., Baniček, M., Demšić, M., Hak, S.: Post-earthquake damage assessment of buildings – procedure for conducting building inspections, GRAĐEVINAR, 72 (2020) 12, pp. 1089-1115, https://doi.org/10.14256/JCE.2969.2020

[22] USGS – United States Geological Survey: Earthquake map: M6.4 - Croatia, 29 December 2020, https://earthquake.usgs.gov/earthquakes/eventpage/us6000d3zh/map, pristupljeno 29. 10. 2025.

[23] Vukobratović, V., Fajfar, P.: Code-oriented floor acceleration spectra for building structures, Bull Earthquake Eng, 15 (2017), pp. 3013–3026, https://doi.org/10.1007/s10518-016-0076-4

[24] HRN EN 19981:2011. Eurokod 8: Projektiranje potresne otpornosti konstrukcija – 1. dio: Opća pravila, potresna djelovanja i pravila za zgrade (EN 1998-1:2004 + AC:2009), Zagreb: Hrvatski zavod za norme, 2011.

[25] HRN EN 1998-3:2011. Eurokod 8: Projektiranje potresne otpornosti konstrukcija – 3. dio: Ocjenjivanje i obnova zgrada (EN 1998-3:2005 + AC:2010), Zagreb: Hrvatski zavod za norme, 2011.

[26] HRN EN 1998-1-1:2024. Eurokod 8: Projektiranje potresne otpornosti konstrukcija – Dio 1-1: Opća pravila i potresna djelovanja (EN 1998-1-1:2024), Zagreb: Hrvatski zavod za norme, 2024.

[27] HRN EN 1998-3:2025. Eurokod 8: Projektiranje potresne otpornosti konstrukcija – 3. dio: Ocjenjivanje i obnova zgrada i mostova (EN 1998-3:2025), Zagreb: Hrvatski zavod za norme, 2025.

[28] Ministero delle Infrastrutture e dei Trasporti. Norme Tecniche per le Costruzioni (NTC 2008). Decreto Ministeriale 14 gennaio 2008. Gazzetta Ufficiale della Repubblica Italiana, n. 29, 4. veljače 2008.

[29] Ministero delle Infrastrutture e dei Trasporti. Norme Tecniche per le Costruzioni (NTC 2018). Decreto Ministeriale 17 januar 2018. Gazzetta Ufficiale della Repubblica Italiana, n. 42, 20. veljače 2018.